

# Surface modification of sulfonated polyvinylchloride cation-exchange membranes by using chitosan polymer containing Fe<sub>3</sub>O<sub>4</sub> nanoparticles

Ehsan Salehi<sup>1</sup> · Sayed Mohsen Hosseini<sup>1</sup> · Saeed Ansari<sup>1</sup> · Alireza Hamidi<sup>1</sup>

Received: 2 September 2015 / Revised: 1 October 2015 / Accepted: 4 October 2015 / Published online: 12 October 2015  
© Springer-Verlag Berlin Heidelberg 2015

**Abstract** Sulfonated polyvinylchloride (SPVC) cation-exchange membranes were coated using chitosan solutions comprising different amounts of Fe<sub>3</sub>O<sub>4</sub> nanoparticles. Influence of chitosan immobilization as well as nanofiller concentration on the electrochemical performance of the membranes was investigated. Electrochemical properties of the membranes including permselectivity, ionic permeability, and areal resistance were studied using an equipped electro dialysis setup and NaCl solution as model electrolyte. Scanning electron microscopy (SEM) and Fourier transform infrared spectroscopy (FTIR) were employed for membrane characterization. Electrochemical performance of the SPVC membranes was improved by coating chitosan polymer. In addition, ionic permeability and permselectivity of the membranes were initially raised by increasing nanoparticles concentration from nil to 2 wt% and then decreased by further insertion of the nanofiller. The areal resistance of the plain SPVC membrane was decreased from 9.4 to 2.9 (ohm) by coating of chitosan solution including optimum value of nano-Fe<sub>3</sub>O<sub>4</sub> due to electrical potential field enhancement across the membrane.

**Keywords** Ion-exchange membrane · Fe<sub>3</sub>O<sub>4</sub> nanoparticles · Coating · SPVC · Chitosan

## Introduction

Membrane technology has attracted increasing attention of researchers especially in progressive engineering fields such as solar cells [1], full cells [2], batteries/capacitors [3], and electro dialysis [4]. Polyvinylchloride-based cation-exchange heterogeneous membranes have been widely used in electro dialysis processes on account of obvious advantages such as favorable electrochemical properties, wide availability, low price, and high mechanical, thermal, and chemical stability [4–6]. Sulfonated polyvinylchloride (SPVC) is SO<sub>3</sub>-functionalized derivative of polyvinylchloride (PVC) polymer with improved properties such as flexibility, durability, and reactivity when compared with the soft PVC [6–8]. Sulfonate functionalities not only can elevate the ion-exchange capacity of the PVC but also provide superior conditions for subsequent chemical modifications if necessary [9]. Moreover, more stable attachment of polymer coatings to the SPVC would be obtained as a result of higher reactivity and increased hydrophilicity of the SO<sub>3</sub>-functionalized polymer.

Nanoparticles have been extensively utilized to enhance the ion-exchange membrane properties such as chemical reactivity, reusability, mechanical durability, thermal resistance, and chemical stability [5, 10–14]. Among popular nanomaterials, nanometal oxides (NMOs) have emerged as highly desirable nanofiller modifiers. NMOs can play important roles in modifying ion-exchange membranes due to their high adsorption capacity, anti-fouling impact, cross-linking mediation, favorable conductivity, biodegradability, and biocompatibility [5, 10, 13]. Titanium dioxide (TiO<sub>2</sub>), zinc oxide (ZnO), iron oxides (Fe<sub>2</sub>O<sub>3</sub> and Fe<sub>3</sub>O<sub>4</sub>), and iron-nickel oxide nanoparticles are examples of NMOs frequently addressed in literature [5, 10, 13, 15].

NMOs can be either incorporated into the polymeric casting solution to obtain mixed-matrix membranes (MMM) or

✉ Ehsan Salehi  
ehsan1salehi@gmail.com

<sup>1</sup> Department of Chemical Engineering, Faculty of Engineering, Arak University, Arak 38156-8-8349, Iran

introduced into the coating solution to modify the membrane surface [16, 17]. The latter modification strategy can be carried out through two distinct ways: perfect coating of modifying layer or local patches of coating material [17]. Internal mass transfer resistances may be somewhat increased when perfect dip-coating is of interest. On the other hand, enhancements in separation performance may not be so convincing by using local coating strategy. Electrochemical properties of cation-exchange membranes can be improved by amino-modification of surface [16, 17]. Amino-functionalization can increase the reactivity of the ion-exchange membrane surface. Enhancement of Donnan potential and water affinity are also attainable by amino-functionalization.

Chitosan (CS) is a biopolymer with broad application in affinity-induced separation processes such as adsorption, chromatography, and ion exchange. Popularity of chitosan is mainly for its favorable hydrophilicity, reactivity, mechanical properties, film-forming capacity, and biocompatibility. CS is a multi-functional hydrophilic polymer with abundant reactive  $-OH$  and  $-NH_2$  functional groups. These functionalities can readily interact with the ions at the membrane surface and enable the polymer to favorably adsorb metal ions from aqueous environment [17–20]. Electrical conductivity of chitosan is not relatively high; however, this polymer can favorably chelate the ions from aqueous environment.

To our knowledge, ion-exchange membranes made of sulfonated PVC have not been ever modified with chitosan solution and iron oxide nanoparticles. The aim of the current study is to study the impacts of chitosan coating as well as nano- $Fe_3O_4$  incorporation into the casting solutions on the electro dialysis performance of the SPVC membranes. Membranes were characterized by using scanning electron microscopy (SEM) microphotography and Fourier transform infrared spectroscopy (FTIR) spectral analysis. Electrochemical properties of the nanocomposite membranes including ionic permselectivity, permeability, and areal resistance were examined using an electro dialysis setup with NaCl solution as model electrolyte.

## Experimental methods and materials

### Chemicals

Polyvinylchloride (PVC, S-7054, supplied by BIPC, Iran) and tetrahydrofuran (THF, 72.11 g/mol, 0.89 g/cm<sup>3</sup>, Merck, Germany) were employed as body polymer and solvent, respectively. Cation-exchange resins (ion exchanger Amberlyst<sup>®</sup> 15, strongly acidic cation exchanger, H<sup>+</sup> form—more than 1.7 mEq/l) and iron oxide nanoparticles ( $Fe_3O_4$ , nanopowder, mean size ~60 nm, SSA >55 m<sup>2</sup>/g, 213.53 g/mol) were obtained from Sigma-Aldrich (USA). Chitosan powder (CS, 100,000–300,000 g/mol, 90 % deacetylated) and polyethylene glycol (PEG,

400 g/mol) were purchased from Acros (USA). All other chemicals were of analytical grades and used as received. Distilled water was used throughout the experiments.

### Membrane preparation

Sulfonated polyvinylchloride was prepared by oxidation of soft polyvinylchloride through batch recirculation with concentrated sulfuric acid. Sulfonation process was carried out according to the procedure proposed by Xu and Kee Lee [7]. Afterwards, SPVC was utilized as the main polymer for the preparation of cation-exchange membranes.

### Support preparation

At first, pristine SPVC membranes were fabricated on the basis of the phase inversion technique. The pristine SPVC membranes were then used as support for the preparation of nanocomposite membranes. Distinct amount of SPVC polymer was dissolved in THF solvent under rigorous stirring (stirrer model: Velp Scientifica Multi 6, USA) for around 7 h. Afterwards, resin particles (–300+400 meshed) were introduced into the polymeric casting solution and sonicated for 1 h using ultrasound bath (SONREX Digit DT52 H, BANDELIN, 240 W, 35 kHz, Germany). After a short period of magnetic restirring, the polymeric solution was casted on clean glass plates using an appropriate applicator. Afterwards, the membranes were dried at room temperature followed by immersing in distilled water as non-solvent agent. Finally, the membranes were soaked in 0.5 M NaCl solution for 48 h to be fully saturated before application in electro dialysis experiments. Membrane thickness was measured using a digital micrometer device (electronic outside micrometer, IP54 model OLR, Lianyungang Linuo Co., China).

### Surface modification

Nanofiller-free casting solution was prepared by dissolving 2 wt% chitosan, 1 wt% polyethylene glycol (as porogen), and 1 wt% acetic acid in DI water under vigorous stirring. Nano- $Fe_3O_4$ -added casting solutions were prepared by introducing different amounts of  $Fe_3O_4$  nanoparticles into the soft CS casting solutions. Nanofiller-added casting solutions were ultrasonicated for around 0.5 h for the desired dispersion of the nanoparticles just before surface modification. Precise slices of SPVC membranes were moisturized and then pasted on clean glass plates for coating. Casting solution was poured onto the surface of the membrane samples and then exactly casted using an applicator with pre-determined gap size of 450  $\mu$ m. Afterwards, the modified membranes were air-dried for 24 h at room temperature and then soaked in 0.5 M NaOH for 1 h to neutralize the excess acid and crosslink. Finally, the resultant membranes were rinsed with abundant

distilled water and saved in 0.5 M NaCl solution for subsequent electro dialysis experiments. Briefly, composition of the resultant membranes is addressed in Table 1.

**Electrodialysis setup**

Electrochemical transport properties of the prepared membranes were examined using a typical two-compartment electro dialysis test cell. The setup has been explained in details elsewhere [4–6]. The membrane sample was sandwiched between the two half-cells and exactly sealed. The half-cells were equipped with platinum electrode supported with a Teflon cover sheet on one side and a porous support for the membrane on the other side. Solutions in both sections were vigorously stirred by magnetic stirrers (in the vicinity of the membrane) to minimize the external mass transfer resistances. The setup was also equipped with electrical power supplier and online data acquisition system.

**Membrane characterization**

*Scanning electron microscopy*

Cross section morphology of the membranes was investigated by using Philips-X130 and Cambridge scanning electron microscopes. In brief, membrane specimens were frozen in liquid nitrogen. Afterwards, the samples were broken and air-dried. The prepared samples were gold sputtered for taking the micrographs in vacuum conditions.

*Fourier transform infrared spectroscopy*

Fourier transform infrared spectroscopy (FTIR) spectral analysis was carried out to specify the functional groups of the polymers and membranes. An ABB Bomem FTIR spectrometer (MB-104) was applied for this purpose.

*Permselectivity*

Membrane potential includes Donnan and diffusion potentials [7, 8]. Ionic permselectivity was computed for the equilibrated membranes by using unbalanced concentrations of NaCl

electrolyte solution ( $C_1=0.1$  M,  $C_2=0.01$  M) on different sides of the membrane in electro dialysis cell. Electrical potential developed across the membrane was monitored by connection of either half-cells to a digital auto multi-meter (DEC, model: DEC 330FC, Digital Multimeter, China) and using saturated calomel electrode through KCl bridges. The membrane potential ( $E_M$ ) is represented by the well-known Nernst equation [21, 22] as

$$E_M = (2t_i^m - 1) \left( \frac{RT}{nF} \right) \ln \left( \frac{a_1}{a_2} \right) \tag{1}$$

where  $t_i^m$  is the transport number of counterions in the membrane phase,  $R$  is the universal gas constant,  $T$  is the absolute temperature,  $n$  is the electrovalence of counterions,  $a_1$  and  $a_2$  are the activities of electrolyte solutions in contact with the membrane surfaces, and  $F$  is the faraday constant. The ion permselectivity of the membranes is represented for the electromigration of counterions through the ion-exchange membrane and given by the following equation [23]:

$$P_s = \frac{t_i^m - t_0}{1 - t_0} \tag{2}$$

where,  $t_0$  is the transport number of counterions in the receiver solution, i.e., solution to that the ions migrate from the feed [21–23].

*Ionic permeability*

Of the setup, 0.1 M NaCl solution was poured in one half-cell and 0.01 M NaCl solution on its other half-cell to measure the ionic permeability of the membranes. DC electrical potential source (Dazheng, DC power supply, Model: PS-302D) with a constant voltage was used across the cell with stable platinum electrodes. Cations can pass through the membrane to appear in cathodic section. Based on the Fick’s first law, flux of the ions can be expressed by [4–7, 23]

$$N = -\frac{V}{A} \times \frac{dC_1}{dt} = P \frac{C_1 - C_2}{d} \tag{3}$$

where  $P$  is the diffusivity of ions,  $d$  is the membrane thickness,  $A$  is the membrane effective area,  $V$  is the volume of the

**Table 1** Composition of coated SPVC cation-exchange membranes

Membrane (abbreviation)	Casting solution composition (Fe <sub>3</sub> O <sub>4</sub> nanoparticles: CS solution) (w/w)
Sample 1 (M)	Pristine (SPVC without coating)
Sample 2 (M0)	0:100 (SPVC with pure CS coating)
Sample 3 (M1)	1:100
Sample 4 (M2)	2:100
Sample 5 (M4)	4:100

Solvent to polymer (THF:SPVC) (v/w) (20:1); resin particles to polymer (resin:SPVC) (w/w) (1:1))

solution,  $C_1$  is the cation concentration in the half-cells, and  $N$  is the ionic flux. Eq. (4) is obtained by integration of Eq. (3) as follows:

$$\ln \frac{(C_1^0 + C_2^0 - 2C_2)}{(C_1^0 - C_2^0)} = -\frac{2PAIt}{Vd} \quad (4)$$

where

$$\begin{aligned} C_1^0 &= 0.1 \text{ M}, C_2^0 = 0.01 \text{ M}, C_1 + C_2 = C_1^0 + C_2^0 \\ &= 0.11 \text{ M} \end{aligned} \quad (5)$$

Diffusion coefficient ( $P$ ) can be calculated by using Eq. (4), where pH variation in cathodic section is being monitored using a digital pH meter (Jenway, model: 3510). Accordingly, flux of the cations can be calculated using Eq. (3).

#### Areal resistance

Electrical resistance of the equilibrated ion-exchange membranes was measured in 0.5 M NaCl solution at ambient temperature. The current bridge was being altered with 1500 Hz frequency (audio signal generator, Electronic Afzar Azma Co. P.J.S) to measure the resistance. The areal resistance was represented by [22]

$$r = R_m \times A \quad (6)$$

where  $r$  is the areal resistance,  $R_m$  is the different between the cell resistance and the electrolyte solution resistance, and  $A$  is the membrane surface area.

## Results and discussion

### Morphology and chemistry

SEM image from the cross section of the plain SPVC membrane is depicted in Fig. 1a. Figure 1b presents the cross section of the CS-coated membranes. The chitosan coating layer with the thickness around 5  $\mu\text{m}$  is obvious in Fig. 1b. Cross section of the CS-coated membranes with 2 wt%  $\text{Fe}_3\text{O}_4$  nanoparticles in the coating layer is shown in Fig. 1c. As it is clear in Fig. 1c, CS layer not only covers the membrane surface homogeneously but also scaffolds the resin agglomerates inside the SPVC membrane matrix. In addition, the coating layer becomes relatively porous as a result of the nanofiller insertion. Microvoids are obvious in chitosan layer in Fig. 1c. It is confirmed by other researchers that morphology plays a pivotal role in electrotransport properties of conductive membranes [24].

Figure 2 shows infrared spectra of PVC and SPVC, respectively. In the measurement results of the soft PVC, the peaks in

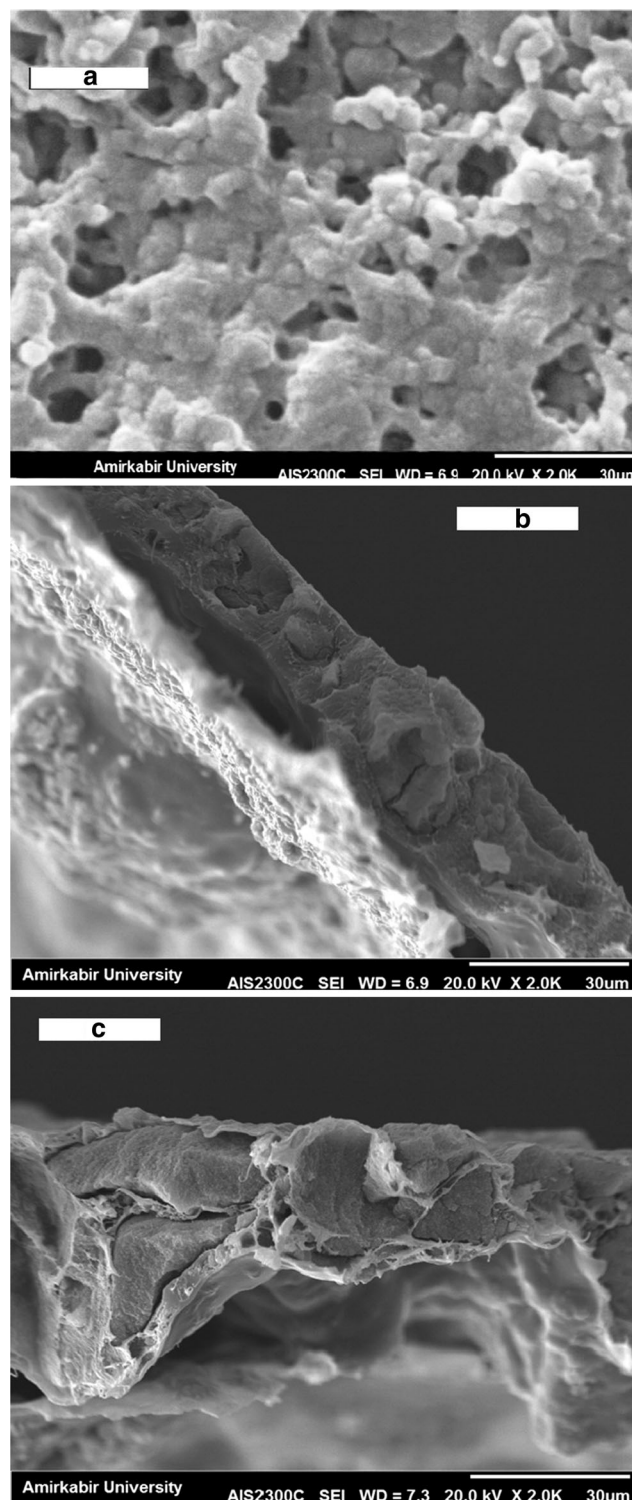


**Fig. 1** Cross section SEM images of **a** pristine SPVC membrane, M ( $\times 1000$  and scale bar 30  $\mu\text{m}$ ), **b** CS-coated SPVC membrane, M0 ( $\times 500$  and scale bar 30  $\mu\text{m}$ ), and **c** CS/ $\text{Fe}_3\text{O}_4$ -coated membrane, M2 ( $\times 500$  and scale bar 30  $\mu\text{m}$ )

the vicinities of 1,425, 959 and 610  $\text{cm}^{-1}$  are peaks originating from the PVC. In many infrared spectra of soft PVC, verification of PVC is accomplished using the C–Cl stretching



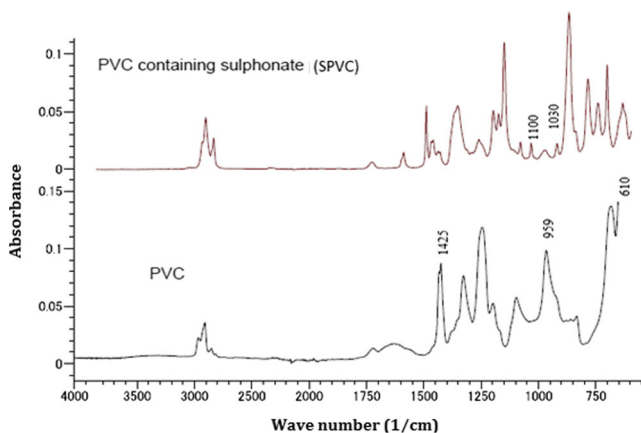


**Fig. 2** Infrared spectra of polyvinyl chloride and sulfonated polyvinyl chloride polymers

vibration near the wavelength of  $610\text{ cm}^{-1}$ . In SPVC spectra, the peaks which appeared around  $1030$  and  $1100\text{ cm}^{-1}$  are ascribed to the symmetric and asymmetric stretching vibration of the sulfonic acid groups [7].

Figure 3 exhibits infrared spectra of pure CS-coated membrane (M0) and CS-coated membrane containing 2 wt%  $\text{Fe}_3\text{O}_4$  nanoparticles (M2). The peak around  $3440\text{ cm}^{-1}$  observed in both curves was ascribed to the vibration of the hydroxyl groups. In the spectrum of CS (Fig. 3 (a)), the absorption bands which appeared at  $1589$  and  $1399\text{ cm}^{-1}$  can be assigned to the N–H bending vibration and C–O stretching bonds of the primary alcohol groups in chitosan polymer. By comparing the infrared spectra of  $\text{Fe}_3\text{O}_4$ –chitosan-coated membranes (Fig. 3 (b)) with that of the pure CS-coated membrane, one can obtain that the  $1589\text{ cm}^{-1}$  peak of the N–H bending vibration shifts to  $1562\text{ cm}^{-1}$ . Moreover, a new peak which appeared at  $560\text{ cm}^{-1}$  connects to the Fe–O group stretching vibrations [25].

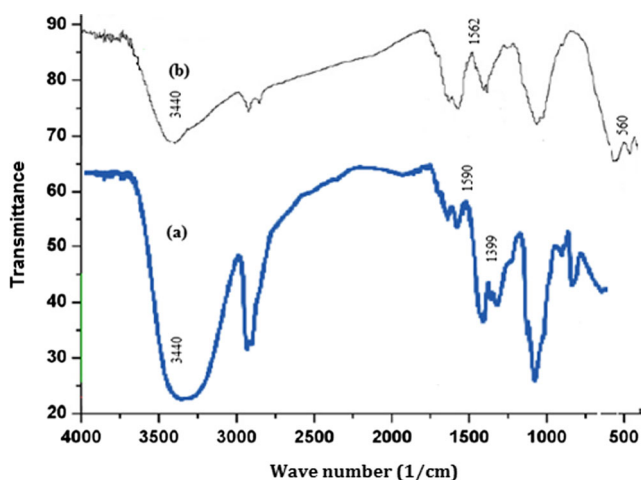


**Fig. 3** Infrared spectra of (a) CS-coated SPVC membrane (M0) and (b) CS/ $\text{Fe}_3\text{O}_4$ -coated SPVC membrane (M2)

## Permselectivity

Selectivity of the cation-exchange membranes originates from the charge that the membrane matrix carries [26]. Result of the NaCl permselectivity through the membranes is depicted in Fig. 4. Results indicate that membrane selectivity is enhanced by coating CS layer. As it is clear in the SEM images, the CS layer covers the membrane surface as well as the resin agglomerates inside the membrane structure for M0 and M2. Chitosan layer can reduce external mass transfer resistances in the vicinity of the membrane surface. Therefore, the ion uptake rate to the membrane surface increases. This may be attributed to the function of the amino and hydroxyl groups of chitosan polymer. Moreover, the membrane surface is provided with more negative charge by hydrolysis of these functional groups. This causes better exclusion of the co-ions (ions of the same charge as the membrane charge) from the membrane surface. Intensification of Donnan potential near the membrane surface resulted from the enhanced exclusion of the co-ions. This fact is the main reason for the improvement of the membrane selectivity. In addition, CS-coated resins can facilitate the transport of the counterions through the membrane matrix [27]. Membrane hydrophilicity is also enhanced as a result of chitosan coating. Thus, the accessibility of the counterions to the fixed sites is facilitated. This also positively affects the transport of the counterions through the membrane [28].

Permselectivity of sodium chloride was further enhanced by introduction of iron oxide nanoparticles in the CS coating layer up to 2 wt%. Membrane selectivity was decreased with further nanoparticle incorporation (from 2 to 4 wt%). Selectivity enhancement may result from the magnetic and adsorptive characteristics of  $\text{Fe}_3\text{O}_4$  nanoparticle toward counterions. Moreover, insertion of  $\text{Fe}_3\text{O}_4$  into the CS layer can also reduce

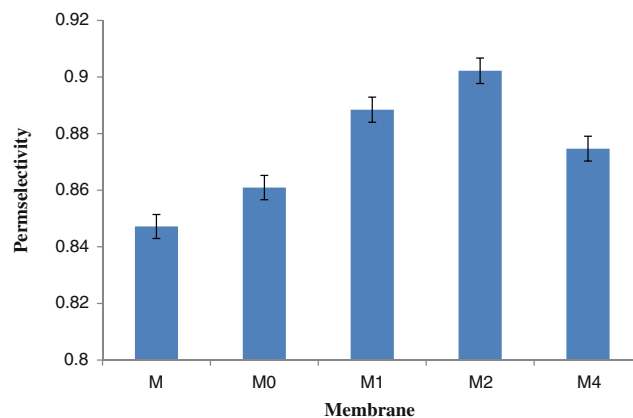


**Fig. 4** Permselectivity of the SPVC cation-exchange membranes with CS coating layer comprising different values of  $\text{Fe}_3\text{O}_4$  nanoparticles

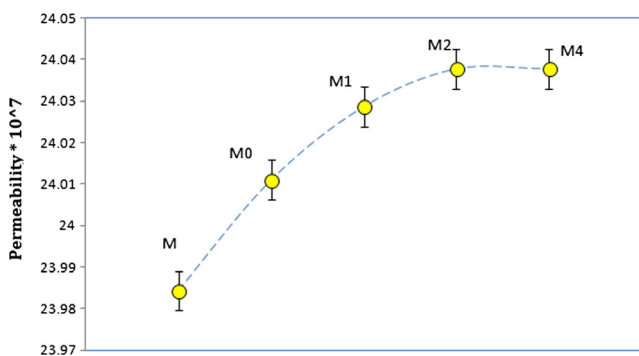


**Fig. 5** Ionic permeability of the CS/Fe<sub>3</sub>O<sub>4</sub> modified SPVC cation-exchange membranes

resistances against transfer of counterions. The observed reduction in the permselectivity at 4 wt%, however, may be attributed to the clogging of the ionic transport pathways. Clogging may be caused by agglomeration of the nanoparticles at high loading contents, as addressed by other researchers [5, 10, 11, 14]. Agglomeration limits the accessibility of the counterions to the reactive sites and thus facilitates the permeation of the co-ions through the membrane. Moreover, increased affinity of Fe<sub>3</sub>O<sub>4</sub> nanoparticles at high additive loading provides the conditions for superior interaction of the ions with the membrane surface. This improves the percolation of the co-ions through the membrane as a result of the concentration gradient development across the membrane.

### Ionic permeability

Permeability of the membranes was improved as a result of the surface modifications (Fig. 5). CS coating layer resulted in ionic flux increase on account of Donnan potential enhancement. Moreover, abundant hydroxyl and amine groups of chitosan are responsible for this behavior [17, 29–31]. Superior monovalent permeability was also obtained by Wang et al. [32], after immobilization of chitosan layer to the bare cation-exchange membrane. Membrane with more negative

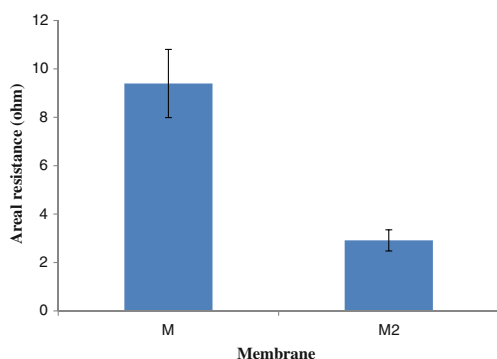


**Fig. 6** Areal resistance of the M (pristine SPVC) and M2 (CS/Fe<sub>3</sub>O<sub>4</sub>) modified SPVC cation-exchange membrane

surface charge can superiorly repel back the co-ions from the membrane surface. Flux of Na<sup>+</sup> ions is also enhanced by the increase of Fe<sub>3</sub>O<sub>4</sub> nanoparticles content in the CS layer. This may be attributed to the adsorptivity of Fe<sub>3</sub>O<sub>4</sub> nanoparticles which strengthens the interactions of the functional sites with the cations [27, 30]. So, the transport of the ions is facilitated in presence of the nanometal oxide. Moreover, the electromagnetic impact of Fe<sub>3</sub>O<sub>4</sub> is also another reason for the permeability improvement. This property causes electrical potential field enhancement across the membrane.

### Areal resistance

The areal resistance experiment is a performance test accompanied with high experimental fluctuations even after many replications. To report meaningful data, only plain SPVC membrane has been compared with the optimal membrane (M2), in this regard. The areal electrical resistance of the optimal and pristine membranes is compared in Fig. 6. It is obvious that the areal resistance is reduced from 9.4 (ohm) in plain membrane to 2.9 (ohm) in CS/Fe<sub>3</sub>O<sub>4</sub>-coated membrane. The electrical resistance is obviously reduced with the help of the CS coating layer and Fe<sub>3</sub>O<sub>4</sub> nanoparticles. This is ascribed to the enhancement of the membrane properties as a result of the CS/nanofiller synergy.

Electromagnetic and adsorptive properties of Fe<sub>3</sub>O<sub>4</sub> nanoparticles can also strengthen the interactions of the ions with the membrane surface. Additionally, Fe<sub>3</sub>O<sub>4</sub> as an efficient mediator for electron transfer can increase the conductivity of the membranes [31–33]. Synergetic effects of CS and the nanofillers would result in enhancement of the electrical potential field across the membrane.

### Conclusions

SPVC heterogeneous cation-exchange membranes were synthesized and then modified with chitosan layer comprising various amounts of Fe<sub>3</sub>O<sub>4</sub> nanofillers. CS layer could enhance electrochemical properties of the membranes by the introduction of plentiful reactive sites on the surface. The ionic flux and permselectivity of the membrane was enhanced by increasing the nanoparticles from nil to 2 wt%. The electrochemical properties were not improved by further additive insertion due to disadvantages of the nanofiller agglomeration. Thus, the optimum nanoparticle content in the CS layer was obtained as 2 wt%. Areal resistance of the membranes was also reduced by CS/Fe<sub>3</sub>O<sub>4</sub> surface modification. Generally, the results indicated that the SPVC membranes modified by CS/Fe<sub>3</sub>O<sub>4</sub> coating are potential candidates for electro dialysis processes.

**Acknowledgments** The authors gratefully acknowledge Arak University for the support during this research.

## References

1. Imperiyka M, Ahmad A, Hanifah SA, Bella F (2014) *Physica B* 450:151–154
2. Hong Neoh C, Zainon Noor Z, Ahmad Mutamim NS, Kim Lim C (2016) *Chem Eng J* 283:582–594
3. Nair JR, Porcarelli L, Bella F, Gerbaldi C (2015) *ACS Appl Mater Interfaces* 7:12961–12971
4. Hosseini SM, Madaeni SS, Heidari AR, Khodabakhshi AR (2012) *Desalination* 285:253–262
5. Hosseini SM, Madaeni SS, Heidari AR, Amirimehr A (2012) *Desalination* 284:191–199
6. Hosseini SM, Gholami A, Madaeni SS, Moghadassi AR, Hamidi AR (2012) *Desalination* 306:51–59
7. Xu L, Kee Lee H (2009) *J Chromatogr A* 1216:6549–6553
8. Mark HF (2004) *Encyclopedia of polymer science and technology*, vol 8, 3rd ed, Wiley, New Jersey, pp 437–476
9. Villaluenga JPG, Barragan VM, Izquierdo-Gil MA, Godino MP, Seoane B, Ruiz-Bauza C (2008) *J Membr Sci* 323:421–427
10. Hosseini SM, Madaeni SS, Khodabakhshi AR, Zendehnam A (2010) *J Membr Sci* 365:438–446
11. Razmjou A, Mansouri J, Chen V (2011) *J Membr Sci* 378:73–84
12. Madaeni SS, Ghaemi N (2007) *J Membr Sci* 303:221–233
13. Vatanpour V, Madaeni SS, Khataee AR, Salehi E, Zinadini S, Ahmadi Monfared H (2012) *Desalination* 292:19–29
14. Li JF, Xu ZL, Yang H, Yu LY, Liu M (2009) *Appl Surf Sci* 255:4725–4732
15. Liang P, Shi T, Li J (2004) *Int J Environ Anal Chem* 84(4):315–321
16. Davis TA, Genders JD, Pletcher D (1997) *A first course in ion permeable membranes*. Publisher: the Electrochemical Consultancy
17. Swaminathan P, Disley PF, Assender HE (2004) *J Membr Sci* 234:131–137
18. Pillai CKS, Paul W, Sharma CP (2009) *Prog Polym Sci* 34:641–678
19. Rutnakornpituk M, Ngamdee P (2006) *Polymer* 47:7909–7917
20. Tang C, Zhang Q, Wang K, Fu Q, Zhang C (2009) *J Membr Sci* 337:240–247
21. Li X, Wang Z, Lu H, Zhao C, Na H, Zhao C (2005) *J Membr Sci* 254:147–155
22. Tanaka Y (2007) *Ion exchange membranes: fundamentals and applications, membrane science and technology series, vol 12*. Elsevier, Netherlands
23. Shahi VK, Thampy SK, Rangarajan R (1999) *J Membr Sci* 158:77–83
24. Kononenko NA, Loza NV, Shkirskaia SA, Falina IV, Khanukaeva DY (2015) *J Solid State Electrochem* 19:2623–2631
25. Kuo CH, Liu YC, Chang CMJ, Chen JH, Chang C, Shieh CJ (2012) *Carbohydr Polym* 87:2538–2545
26. Razmjou A, Resosudarmo A, Holmes RL, Li H, Mansouri J, Chen V (2012) *Desalination* 287:271–280
27. Shuang C, Wang M, Zhou Q, Zhou W, Li A (2013) *Water Res* 47:6406–6414
28. Nagarale RK, Gohil GS, Shahi VK, Rangarajan R (2004) *Colloids Surf A Physicochem Eng Asp* 251:133–140
29. Salehi E, Madaeni SS (2014) *Appl Surf Sci* 288:537–541
30. Daraei P, Madaeni SS, Ghaemi N, Salehi E, Khadivi M, Moradian R, Astinchap B (2012) *J Membr Sci* 415/416:250–259
31. Salehi E, Madaeni SS, Rajabi L, Derakhshan AA, Daraei S, Vatanpour V (2013) *Chem Eng J* 215–216:791–801
32. Wang M, Jia Y, Yao T, Wang K (2013) *J Membr Sci* 442:39–47
33. Antolini E (2015) *Biosens Bioelectron* 69:54–70